

Article

Application of Dual Frequency Comb Method as an Approach to Improve the Performance of Multi-Frequency Simultaneous Radiation Doppler Radar for High Temperature Plasma Diagnostics

Tokihiko Tokuzawa ^{1,2,*} , Shigeru Inagaki ³ , Michiaki Inomoto ⁴ , Akira Ejiri ⁴, Tatsuhiro Nasu ², Toru Ii Tsujimura ¹ and Katsumi Ida ^{1,2}

¹ National Institutes of Natural Sciences, National Institute for Fusion Science, Toki 509-5292, Japan; tsujimura.tohru@nifs.ac.jp (T.I.T.); ida.katsumi@nifs.ac.jp (K.I.)

² Department of Fusion Science, The Graduate University for Advanced Study, SOKENDAI, Toki 509-5292, Japan; nasu.tatsuhiro@nifs.ac.jp

³ Institute of Advanced Energy, Kyoto University, Gokasho, Uji 611-0011, Japan; inagaki.shigeru.7s@kyoto-u.ac.jp

⁴ Graduate School of Frontier Sciences, The University of Tokyo, Kashiwa 277-8561, Japan; inomoto@k.u-tokyo.ac.jp (M.I.); ejiri@edu.k.u-tokyo.ac.jp (A.E.)

* Correspondence: tokuzawa@nifs.ac.jp

Featured Application: Plasma science, Fusion reactor.



Citation: Tokuzawa, T.; Inagaki, S.; Inomoto, M.; Ejiri, A.; Nasu, T.; Tsujimura, T.I.; Ida, K. Application of Dual Frequency Comb Method as an Approach to Improve the Performance of Multi-Frequency Simultaneous Radiation Doppler Radar for High Temperature Plasma Diagnostics. *Appl. Sci.* **2022**, *12*, 4744. <https://doi.org/10.3390/app12094744>

Academic Editor: Ernesto Limiti

Received: 12 April 2022

Accepted: 5 May 2022

Published: 8 May 2022

Publisher's Note: MDPI stays neutral with regard to jurisdictional claims in published maps and institutional affiliations.



Copyright: © 2022 by the authors. Licensee MDPI, Basel, Switzerland. This article is an open access article distributed under the terms and conditions of the Creative Commons Attribution (CC BY) license (<https://creativecommons.org/licenses/by/4.0/>).

Abstract: A new Doppler radar using millimeter-waves in the Ka-band, named the “dual-comb Doppler reflectometer”, has been developed to measure the turbulence intensity and its velocity in high-temperature plasmas. For the realization of a fusion power generation, it is very important to know the spatial structure of turbulence, which is the cause of plasma confinement degradation. As a non-invasive and high spatial resolution measurement method for this purpose, we apply a multi-frequency Doppler radar especially with simultaneous multi-point measurement using a frequency comb. The newly developed method of synchronizing two frequency combs allows a lower intermediate frequency (IF) than the previously developed frequency comb radar, lowering the bandwidth of the data acquisition system and enabling low-cost, long-duration plasma measurements. In the current dual-comb radar system, IF bandwidth is less than 0.5 GHz; it used to be 8 GHz for the entire Ka-band probing. We applied this system to the high-temperature plasma experimental device, the Large Helical Device (LHD), and, to demonstrate this system, verified that it shows time variation similar to that of the existing Doppler radar measurements.

Keywords: millimeter-wave; frequency comb; Doppler reflectometer; DBS; LHD

1. Introduction

Doppler radar, which measures the Doppler shift of reflected and scattered waves from moving objects to determine their velocity, has been used in various fields, and has also been applied to velocity measurement of turbulent flow in high-temperature plasma. Since electromagnetic waves in the millimeter-wave range can be used in relation to the electron plasma frequency and the electron cyclotron frequency range, the system is expected to be used as a stable and robust measurement method, and is also expected to be used in future nuclear burning fusion reactors. In fusion plasma research, this Doppler radar is called a Doppler reflectometer or a Doppler back-scattering and has been applied to various experimental devices around the world, such as helical/stellarators (Wendelstein 7-AS [1,2], 7-X [3], TJ-II [4], LHD [5–8]), tokamaks (Tuman-3M [9], ASDEX Upgrade [10–13], Tore Supra [14,15], DIII-D [16,17], JT-60U [18], MAST [19], JET [20], HL-2A [21], TCV [22], EAST [23–25]), and linear

machines (C-2 FRC [26], GAMMA-10 [27]). In particular, in recent years, systems capable of simultaneous multi-frequency observation have been developed with the aim of understanding the instantaneous spatial structure of turbulence [6–8,13,17,21–25]. When observing turbulence in torus plasmas with this Doppler reflectometer, an ordinary or extraordinary wave is injected into the magnetic confined plasma, and the back-scattered wave from the vicinity of the cut-off position corresponding to the injecting frequency is observed, so the measurement position can be changed by changing the frequency. Therefore, it is necessary to inject electromagnetic waves of different frequencies to obtain information at various radial positions in the plasma.

This multi-frequency measurement technique has been studied and developed in various ways, as shown in Figure 1. The first is to prepare multiple millimeter-wave sources with fixed frequencies and inject them together [28–30]. This is the most robust method, but it is difficult to increase the number of frequencies significantly, due to the need to prepare many millimeter-wave sources and to mix signals. The second method is to vary the frequency [3–5,10–12,14–16,18–20]. This method has the advantage of requiring only one set of millimeter-wave sources as hardware and is relatively easy to calibrate. The method of varying frequencies in a staircase fashion is called frequency hopping, and is also used for zonal flow measurement with high spatial resolution [20]. The disadvantage of this method is that it does not allow instantaneous measurements. If fast plasma changes, such as transition phenomena, occur within the time required for the frequency sweep, it becomes difficult to understand the spatial structure. Another method is to sweep the frequency continuously to obtain the density profile with high temporal resolution, and then extract the fluctuation component by calculation [31]. The third method is to use pulsed electromagnetic waves as a source [32–34]. This method, called ultrashort pulse radar, uses the broad frequency component of the pulse to ensure a wide bandwidth. The disadvantages of this method are the limited time resolution and the relative complexity of the system. For example, the repetition rate of conventional pulse output is up to about 1 MHz. The time-of-flight instrument used in this method requires a large number of filter banks for received signal processing in order to improve spatial resolution. The fourth method is to use a frequency comb [6–8,17]. The advantages of this method are that it can utilize the intermittent but broad frequency components of a single frequency comb output, and the repetitive oscillation frequency can be increased to several hundred MHz or more, allowing it to be handled like a pseudo-continuous wave. In other words, a simple measurement system using a single source can extract a broad frequency component and achieve high spatial and temporal resolution at the same time. A frequency comb is a signal with periodic peak frequency components and utilizes oscillation from a single source such as a non-linear transmission line (NLTL) or step recovery diode (SRD), as shown in Figure 2, or comb-like frequency component radiation using a multiplier [13,21–25].

Recently, we have been applying frequency comb Doppler reflectometers in the LHD [6,8], and the precise radial profiles of the perpendicular velocity are obtained up to 20–40 radial points, simultaneously, by using a high sampling rate (80 GS/s) data acquisition system. This is a very useful technique, but the observation time is limited due to the limitation of the stored memory. To solve this problem by slowing down the sampling rate, we try to reduce the intermediate frequency (IF) components in the mixer output of the heterodyne detection circuit. In addition, if the IF frequency can be lowered, not only can the sampling rate be reduced, but the frequency bandwidth of the filter bank can also be lowered. This makes it easier to reduce the associated component costs, add more frequency channels, and improve spatial resolution.

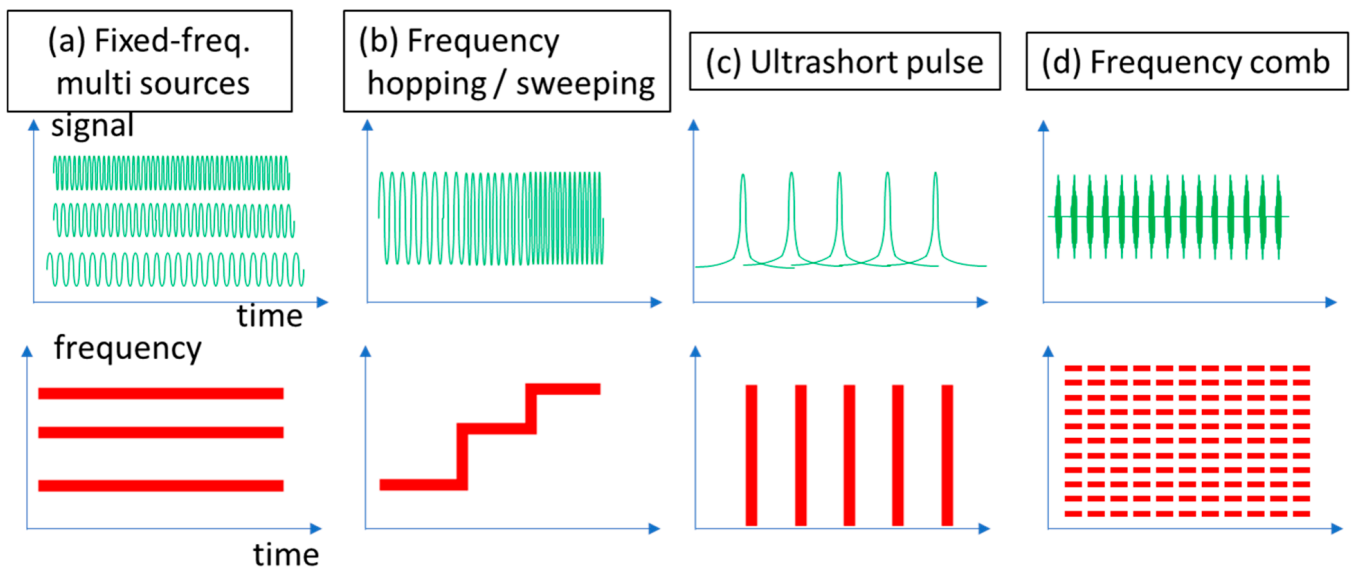


Figure 1. Schematic diagram of various methods of multi-frequency reflectometer technology. Images of temporal behavior of output signal wave forms (green) and frequencies (red). (a) Different fixed frequency sources method utilizes independent continuous wave with different frequency components. (b) Frequency hopping or frequency sweeping method utilizes time varying frequencies. (c) Ultrashort pulse method utilizes a train of impulse which has broadband frequency component. (d) Frequency comb method utilizes simultaneous discrete frequency components.

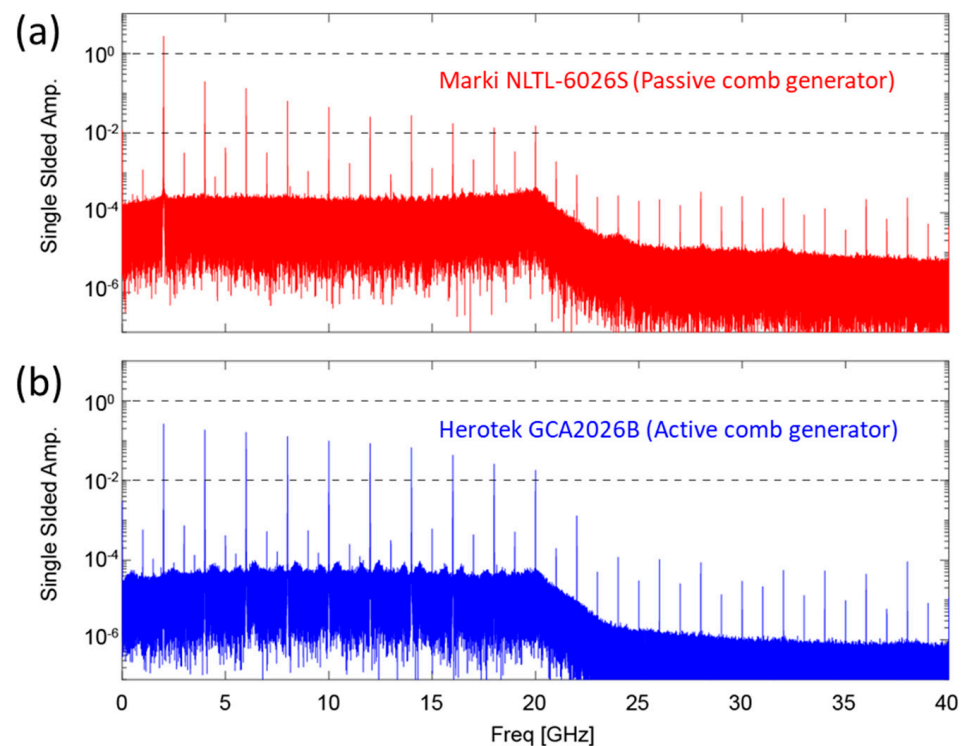


Figure 2. Examples of frequency spectrum of different frequency comb sources: (a) Marki Microwave, Inc. model: NLTL-6026S (b) Herrotek, Inc. model: GCA2026B. Both comb sources are controlled to output frequency components every 2 GHz. Here, the spectral power degradation in the region above 20 GHz is due to the frequency bandwidth limitation, since the data was collected by an oscilloscope with a bandwidth of 20 GHz and a sampling rate of 80 GS/s.

In this paper we report on the development of a new Doppler reflectometer system based on a frequency comb source and the results of a demonstration experiment in which it was applied to an LHD plasma. Section 2 introduces the principle of the Doppler reflectometer, and Section 3 describes the dual-comb system using two frequency comb sources, which contributes to various cost reductions, and explains the operating principle. Section 4 describes the dual-comb Doppler reflectometer system for LHD plasma measurement and describes the results of its operational tests and initial plasma demonstration observation.

2. Principle of Doppler Reflectometer for Fusion Plasma Science

Nowadays, Doppler reflectometry (also called Doppler back-scattering: DBS) is a powerful diagnostic tool for plasma turbulence studies, because it can measure the perpendicular velocity of electron density fluctuations v_{\perp} , the radial electric field E_r , and the perpendicular wavenumber spectrum $S(k_{\perp})$ in high-temperature magnetized confinement plasmas with high spatial and temporal resolution.

The principle of Doppler reflectometry in the toroidal plasma measurements is explained simply as follows. When a probing microwave/millimeter-wave beam is injected into a plasma and approaches a cut-off layer with an oblique angle to the cut-off surface, a back-scattering occurs, caused by the density fluctuations which matches the Bragg condition, i.e., $k = -2 k_i$ (where k_i is the local wave vector of the launching beam). The power of the back-scattered radiation is proportional to the density fluctuation amplitude, that is, $P_s \propto |\tilde{n}_e|^2$. In addition, when the fluctuations move with a velocity \mathbf{v} , the back-scattered signal shows a Doppler frequency shift $2\pi f_D = \mathbf{v} \cdot \mathbf{k} \approx v_{\perp} k_{\perp}$. Figure 3 shows the example of the frequency spectrum obtained in the LHD plasma experiment. The frequency broadening caused by the density fluctuation and the Doppler shift is clearly observed. In addition, the frequency component of 1.86 GHz is the IF frequency down-converted from the carrier wave. The perpendicular velocity is a composition of the plasma background $\mathbf{E} \times \mathbf{B}$ velocity v_{ExB} and the intrinsic phase velocity of the density fluctuations v_{ph} , and this composition is given as $v_{\perp} = v_{ExB} + v_{ph}$. If v_{ph} is known or $v_{ph} \ll v_{ExB}$ (which is usually satisfied at the plasma edge in magnetized confinement toroidal plasmas), the radial electric field E_r can be extracted. The rapid change of E_r and its radial structure is considerable in playing an important role in plasma confinement, such as the H-mode transition. Therefore, simultaneous measurement of multiple spatial points is required.

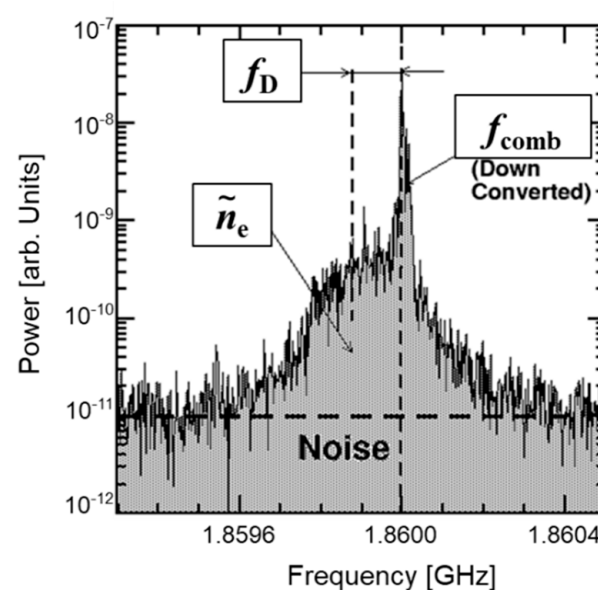


Figure 3. Example of Doppler shift frequency spectrum obtained by reflectometer in LHD. Here, $f_{\text{comb}} = 1.86$ GHz is IF frequency down-converted from carrier wave and f_D is estimated Doppler shift frequency.

3. Concept of Dual-Comb Operation

A frequency comb is a radiation source that can generate many peaked frequency components simultaneously, making it suitable as a probe source for simultaneous multipoint measurements with a Doppler reflectometer. The most important issue in multi-frequency simultaneous measurement is the receiving technique, which requires multiple filter banks and detectors to differentiate and measure multiple frequencies, which increases the cost. Another technique, other than filter banks, is to collect all components of the frequency comb with a wideband digitizer and apply digital signal processing. In this case, however, it is difficult to collect data for a long-time duration due to memory issues. To reduce these problems, the dual-comb system was devised. To illustrate the concept, the following is an example of a probing range in the Ka-band (26.5–40 GHz). As shown in Figure 4, the Probe signal generated by a frequency comb has multiple frequency peaks with a bandwidth of about 14 GHz. When the Local frequency is set outside the Ka-band, the down-converted intermediate frequency (IF) bandwidth is also about 14 GHz, as shown in Figure 4a. When the Local frequency is exquisitely shifted from the peak near the center value of the Probe frequency range, the IF frequency bandwidth can be reduced by about half, as shown in Figure 4b. By setting the Local frequency in this way, the previously developed measurement system [6,8] could be applied to plasma measurements. Is there any way to lower the IF bandwidth? We have devised a new method for this project. That is the dual-comb method. Thereby, a frequency comb is used not only for the Probe signal, but also for the Local signal, as shown in Figure 4c. It is important to note that the clock (fundamental) frequencies of these two frequency combs are slightly offset. In this way, the IF bandwidth is expected to be significantly reduced to about 0.5 GHz.

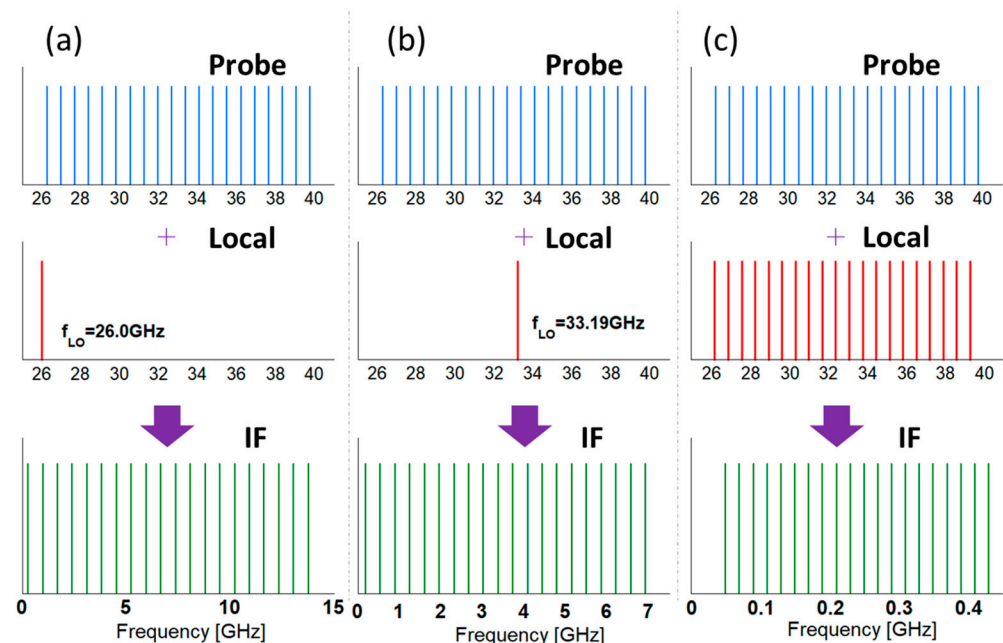


Figure 4. Schematic diagram of generating IF frequency. The blue (top), red (middle), and green (bottom) lines indicate the frequency components of probing comb, local, and IF, respectively. Here, frequency band of RF probe depicted as Ka-band. (a) Local frequency set outside RF frequency range. (b) Local frequency set near center RF frequency range. (c) Dual comb cases. Here, frequency difference between probe and local source drawn with 10 MHz shift.

A confirmation test was conducted to see if the IF could actually be lowered. The conceptual test circuit shown in Figure 5 was built and the frequency spectrum was observed. The frequency combs created with a 190 MHz (f_1) clock and a 200 MHz (f_2) clock are input to the mixer as RF and LO, respectively. If m and n are integers greater than or equal to 0, the mixer outputs $|mf_1 - nf_2|$ frequency components. Therefore, the

mixing frequencies of RF and LO comb components that are closest each other would line up at 10 MHz intervals. The frequency spectrum of this test is shown in Figure 5c. Thus, it was confirmed that the dual-comb method can generate discrete IF components at each frequency step, and that IF bandwidth reduction can be achieved.

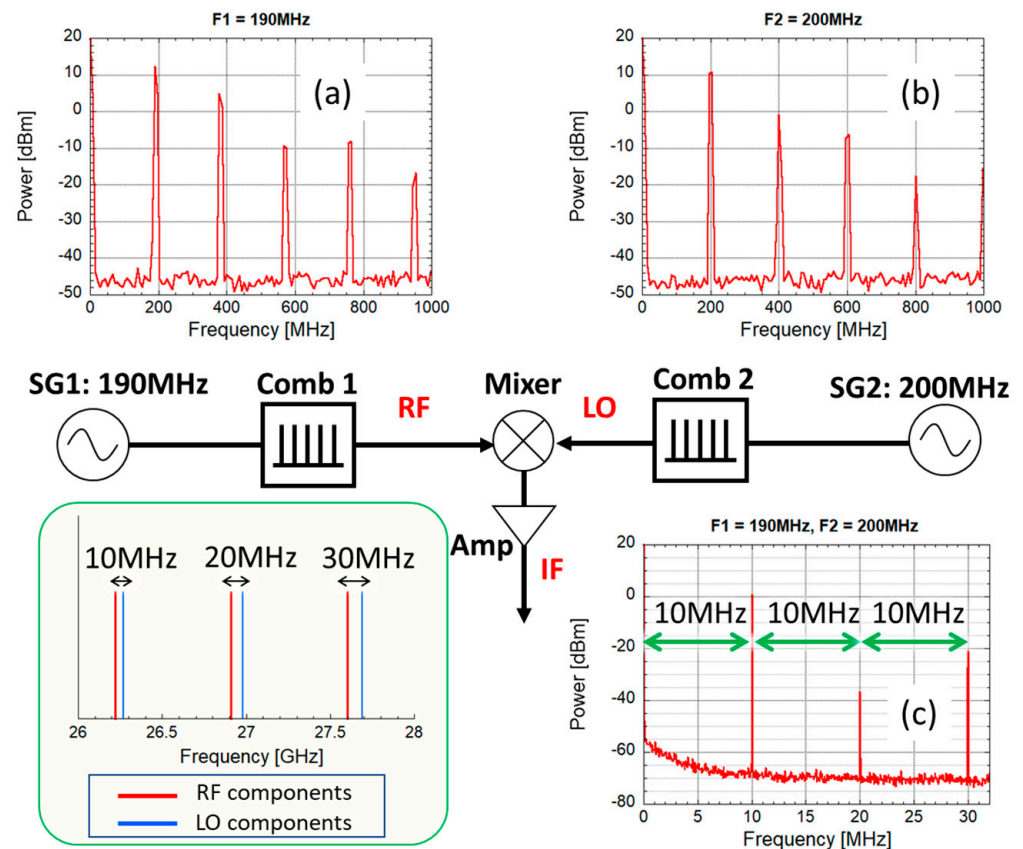


Figure 5. Schematic diagram of dual comb operation concept. Here, signal generators (SGs) of SG1 (190 MHz) and SG2 (200 MHz) are used as clocks for comb generation for RF and LO, respectively. Frequency spectra: (a) RF, (b) LO, and (c) IF signals observed in this conceptual test.

4. Dual-Comb Doppler Reflectometer System in LHD

4.1. System Equipment

The Ka-band dual-comb Doppler reflectometer system is shown in Figure 6. The comb sources are operated by 710 and 730 MHz, respectively. A frequency of 710 MHz is chosen because the RF frequencies of the probing match the frequencies of the previous Doppler reflectometer system [6,8] to make correlative measurements at two separate toroidal locations. Output frequency spectrum of the comb generator is shown in Figure 7a. The output power is approximately flat, up to >20 GHz. Of these frequency components, only the 12–20 GHz components are extracted by the bandpass filter (BPF), as shown in Figure 7b, and the frequencies are doubled to obtain the probing Ka-band components, as shown in Figure 7c. Note that the frequency interval after doubling is f_1 , not $2f_1$. One of the frequency comb components is selected to use the LO of the Mixer 1 by BPF of 26.27 GHz with ± 150 MHz bandwidth, as shown in Figure 7d. Then, the output of Mixer 1 is combined with the different frequency comb components from Comb Generator 2 at Mixer 3 and generates the “Probe signal”. For the precise heterodyne detection, a part of each signal from Comb Generator 1 and Comb Generator 2 components are mixed in Mixer 2 and generate the frequency chain which is used for the “Reference signal” for IQ detection [6]. The test results of the IQ detection system, performed using a reflector instead of plasma, are shown in Figure 8. First, the frequency components for IQ detection are extracted from

the probe and reference signals (Figure 8a) by filter banks. Here, the 120 MHz signal is shown in Figure 8b as an example. Next, the IQ output is used to calculate the complex signal and the phase difference between the probe and reference signals at each frequency component. As shown in Figure 8c, when a phase change was applied to the RF probe signal as a test, the IQ signal output changed correctly, indicating that this IQ detection system is working properly.

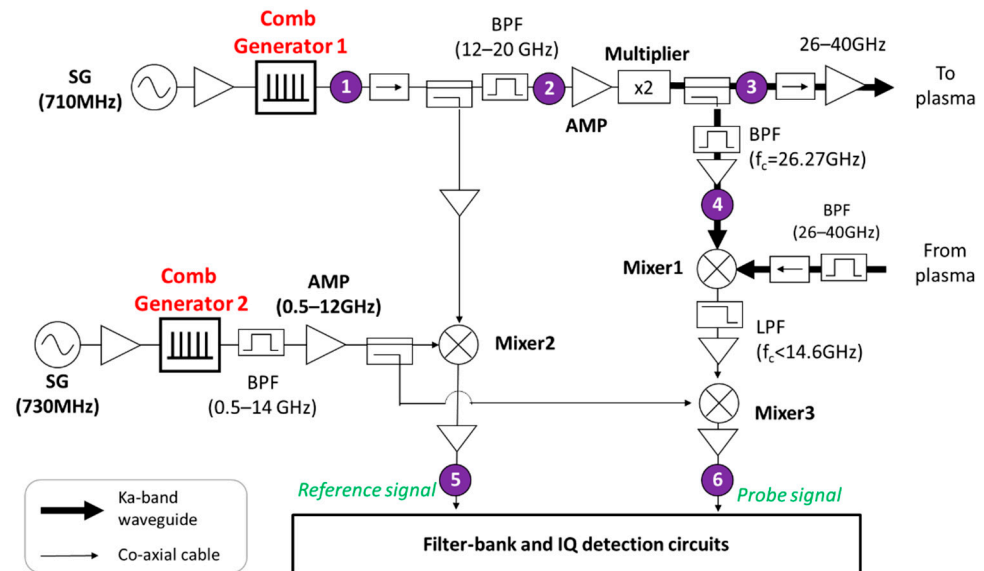


Figure 6. Schematic diagram of Ka-band dual-comb Doppler reflectometer system. Here, SG is signal generator used as clock for comb generation, AMP is amplifier, BPF is band-pass filter, and LPF is low-pass filter. Numbers 1, 2, 3, 4, 5, 6 in figure indicate monitoring points in following figures.

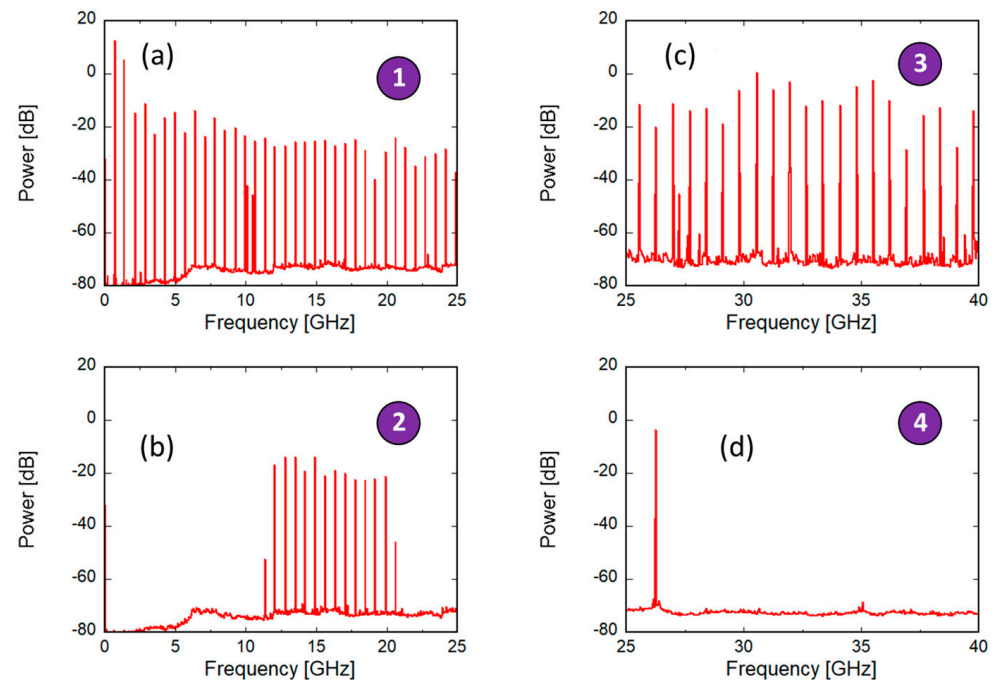


Figure 7. Frequency spectra of (a) output of comb generator (monitor point of 1), (b) output through bandpass filter (monitor point of 2), (c) output of multiplier which generates Ka-band frequency components (monitor point of 3), and (d) Local signal for Mixer 1 (monitor point of 4).

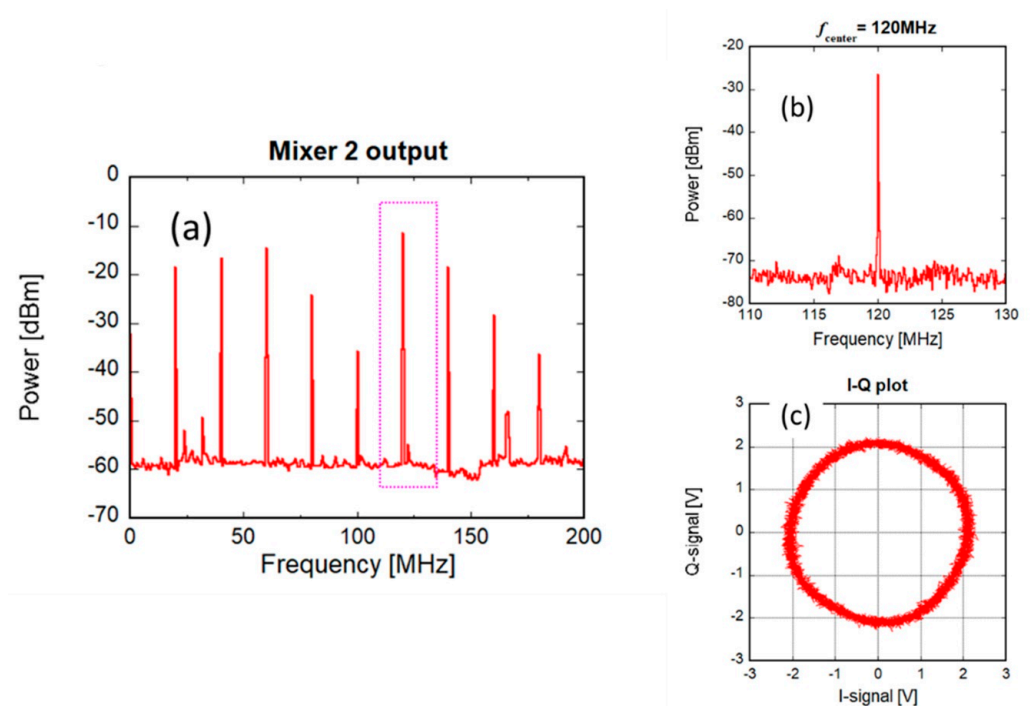


Figure 8. Frequency spectra of reference signal of IQ detection circuit (monitor point 5). (a) Entire reference signal and (b) 120 MHz component of a portion of the figure in (a) (the area enclosed by the dotted square) enlarged. (c) Example of phasor plot (In-phase and Quadrature-phase).

In addition, the frequency comb output injected into the plasma should be flat or have a strong high frequency component, and we would like to investigate ways to improve the structure of this frequency intensity in the future.

4.2. System Test for Doppler Shift Measurement by Rotating Grating

The most attractive feature of Doppler radar is its ability to measure the velocity of a target object. We conducted a test to confirm whether this dual-comb Doppler reflectometer system can observe the velocity of an object. For this test, a grating drum with a diameter of 500 mm and a grating spacing of 10 mm was prepared, as shown in Figure 9a. Its rotational speed is variable up to 800 rpm by the controller. The relationship between the drum rotation speed ω and the Doppler shift frequency f_D can be expressed by $f_D = r\omega \cdot 2k \sin \theta / 2\pi$. Here, r (=250 mm) is the drum radius and θ (=45 degrees) is the angle of incidence with respect to the normal drum surface, as shown in Figure 9b.

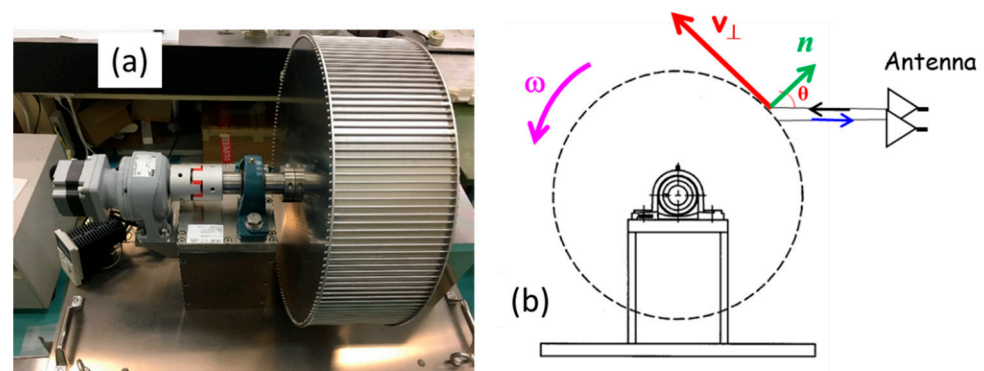


Figure 9. (a) Photograph of rotating grid drum and (b) Schematic layout of the test for the Doppler shift measurement.

The received signal of Mixer 3 clearly shows the discrete peaks associated with the grating structure and the spectral frequency shift associated with the rotating drum, as shown in Figure 10a. A Gaussian fit is applied to the observed frequency spectrum to estimate the Doppler shift frequency. The obtained Doppler shift frequencies at different rotating speeds of the drum, are shown in Figure 10b. The linear relationship expected from the above equation is clearly observed, indicating that Doppler shift measurement is possible in this dual-comb system.

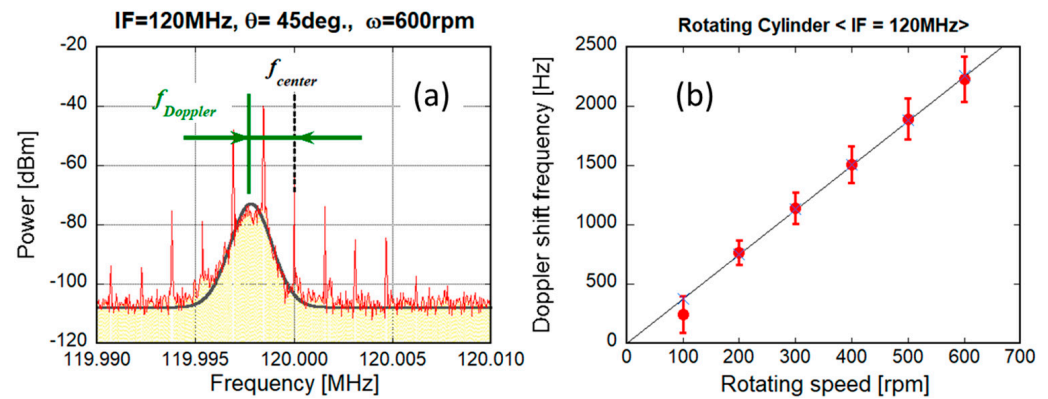


Figure 10. (a) Example of frequency spectrum of signal scattered from rotating drum whose rotating speed is 600 rpm. Black line is result of Gaussian fitting. (b) Estimated Doppler shift frequency as function of rotating speed of drum. Black dotted line is the line estimated from equation $f_D = r\omega \cdot 2k \sin \theta / 2\pi$.

4.3. First Observation in LHD Plasma

The dual-comb Doppler reflectometer system is installed in the LHD to measure the turbulent plasma velocity in the high-temperature plasma experiment. This is carried out under the condition that the magnetic axis position in the vacuum field is $R_{ax} = 3.60$ m, the magnetic field strength is $B_t = 2.75$ T, the helical coil pitch parameter $\gamma = 1.2538$, and the ratio of the quadrature field $B_q = 100\%$. For plasma heating, 5 MW ECH and 15 MW NBI are used. During the plasma discharge (which shot number is #148725) the electron temperature is kept above 1.0 keV. The example of the frequency spectrum of the observed scattered signal is shown in Figure 11a. This spectrum is obtained by performing FFT processing on 2^{22} (=4,194,304) data points of the Mixer 3 output signal, collected by a wideband digital oscilloscope. Some visible peaks in the figure correspond to the injected frequency comb components. Figure 11b is the enlarged view of one frequency comb component with an IF frequency of 120 MHz. The center frequency of 120 MHz in this spectrum corresponds to the 30.5 GHz carrier frequency component injected into the plasma in this frequency comb system. A clear frequency shift due to the presence of plasma turbulence is observed. The time variation of the Doppler shift frequency can be obtained by IQ detection using the method in Reference 10. The plasma flow velocity can then be estimated from this Doppler shift frequency. Figure 12 shows the plasma flow velocity estimated by the Doppler reflectometer in this plasma discharge, where the plasma is initiated by ECH at $t = 3.3$ s and additional heating is provided by perpendicular NBI (p -NBI) and tangential NBI (t -NBI). The change in flow velocity can be observed in response to changes in the plasma state. The observed signal agrees well with that obtained from the different Doppler reflectometer, using a frequency hopping method [5] which uses the same antenna, indicating that the dual comb system can be used to measure the plasma flow velocity.

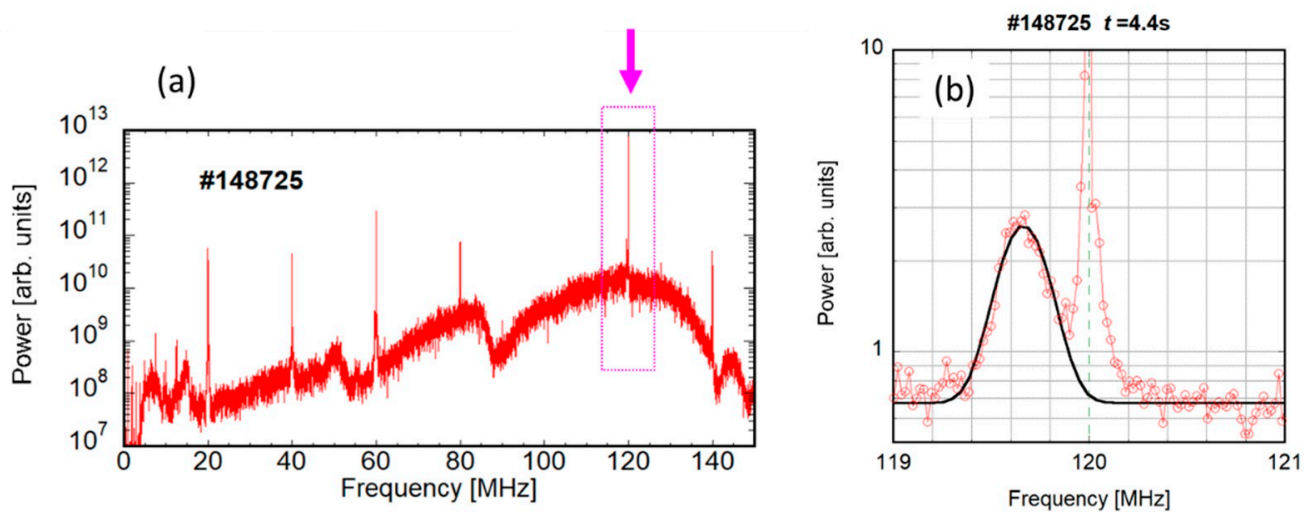


Figure 11. Frequency spectra of (a) entire scattered signal from LHD plasma (shot number is #148725). and (b) magnified view of 120 MHz IF frequency component (the area enclosed by the dotted square in (a)). (monitor point 6).

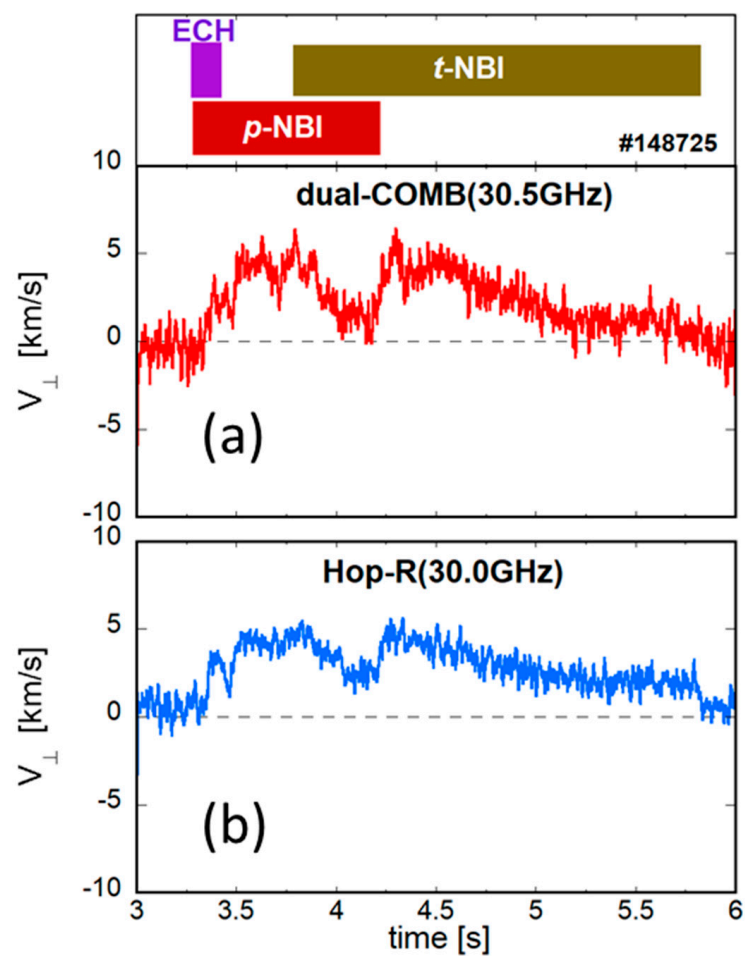


Figure 12. Temporal behavior of plasma perpendicular flow velocity obtained with (a) dual comb system at 30.5 GHz and (b) frequency-hopping Doppler reflectometer system operated at fixed 30.0 GHz, respectively. Shot number of LHD plasma is #148725. The injection timing of heating power for ECH, p-NBI, and t-NBI is shown above in color bar.

5. Conclusions

A Ka-band dual-comb Doppler reflectometer has been developed to simultaneously measure turbulence intensity and its velocity in high-temperature plasmas at multiple spatial points. This dual-comb method has the potential to significantly reduce the IF frequency, compared to the conventional frequency comb method. Using this method, we confirmed that the velocity of a rotating object can be observed as a Doppler shift on a rotating drum on a test bench. We applied this method to LHD plasma measurements and conducted a demonstration experiment using high-temperature plasma to show that plasma flow velocity can be measured using this dual-comb method.

In the future, this system will perform more multi-point measurements in the LHD, and we hope to present the results soon. Furthermore, the frequency comb technique is expected to apply not only to Doppler reflectometry, but also to other radar systems such as density profile measurements, as in reference [35].

Author Contributions: Conceptualization, T.T.; methodology, T.T. and S.I.; validation, T.T., T.N. and T.I.T.; investigation, M.I.; writing—original draft preparation, T.T.; writing—review and editing, T.T. and A.E.; funding acquisition, T.T. and K.I. All authors have read and agreed to the published version of the manuscript.

Funding: This work was partially supported in part by KAKENHI (Nos. 21H04973, 19H01880, 17K18773, 17H01368, 15H02335 and 15H02336), by a budgetary Grant-in-Aid from the NIFS LHD project under the auspices of the NIFS Collaboration Research Program (ULPP027, KLPH024, and KBAP066), by the collaboration programs of the RIAM of Kyushu University, and by the Asada Science foundation.

Institutional Review Board Statement: Not applicable.

Informed Consent Statement: Not applicable.

Data Availability Statement: Data can be accessed from the Large Helical Device (LHD) data repository server of National Institute for Fusion Science (NIFS) at https://www-lhd.nifs.ac.jp/pub/Repository_en.html (accessed on 19 December 2018).

Acknowledgments: The authors would like to thank the technical staff of the LHD for their support for these experiments and appreciate the advice provided through the U.S.-Japan Fusion Research and Development Cooperation.

Conflicts of Interest: The authors declare no conflict of interest.

References

1. Hirsch, M.; Holzhauer, E.; Baldzuhn, J.; Kurzan, B.; Scott, B. Doppler reflectometry for the investigation of propagating density perturbations. *Plasma Phys. Control. Fusion* **2001**, *43*, 1641. [\[CrossRef\]](#)
2. Hirsch, M.; Holzhauer, E.; Baldzuhn, J.; Kurzan, B. Doppler reflectometry for the investigation of propagating density perturbations. *Rev. Sci. Instrum.* **2001**, *72*, 324. [\[CrossRef\]](#)
3. Windisch, T.; Wolf, S.; Weir, G.M.; Bozhenkov, S.A.; Damm, H.; Fuchert, G.; Grulke, G.; Hirsch, M.; Kasperek, W.; Klinger, T.; et al. Phased array Doppler reflectometry at Wendelstein 7-X. *Rev. Sci. Instrum.* **2018**, *89*, 10E115. [\[CrossRef\]](#) [\[PubMed\]](#)
4. Happel, T.; Estrada, T.; Blanco, E.; Tribaldos, V.; Cappa, A.; Bustos, A. Doppler reflectometer system in the stellarator TJ-II. *Rev. Sci. Instrum.* **2009**, *80*, 073502. [\[CrossRef\]](#) [\[PubMed\]](#)
5. Tokuzawa, T.; Ejiri, A.; Kawahata, K.; Tanaka, K.; Yamada, I.; Yoshinuma, M.; Ida, K.; Suzuki, C. Microwave Doppler reflectometer system in LHD. *Rev. Sci. Instrum.* **2012**, *83*, 10E322. [\[CrossRef\]](#)
6. Tokuzawa, T.; Inagaki, S.; Ejiri, A.; Soga, R.; Yamada, I.; Kubo, S.; Yoshinuma, M.; Ida, K.; Suzuki, C.; Tanaka, K.; et al. Ka-band Microwave Frequency Comb Doppler Reflectometer System for the Large Helical Device. *Plasma Fusion Res.* **2014**, *9*, 1402149. [\[CrossRef\]](#)
7. Soga, R.; Tokuzawa, T.; Watanabe, K.Y.; Tanaka, K.; Yamada, I.; Inagaki, S.; Kasuya, N. Developments of frequency comb microwave reflectometer for the interchange mode observations in LHD plasma. *J. Instrum.* **2016**, *11*, C02009. [\[CrossRef\]](#)
8. Tokuzawa, T.; Tsuchiya, H.; Tsujimura, T.; Emoto, M.; Nakanishi, H.; Inagaki, S.; Ida, K.; Yamada, H.; Ejiri, A.; Watanabe, K.Y.; et al. Microwave frequency comb Doppler reflectometer applying fast digital data acquisition system in LHD. *Rev. Sci. Instrum.* **2018**, *89*, 10H118. [\[CrossRef\]](#)
9. Bulanin, V.V.; Lebedev, S.V.; Levin, L.S.; Roytershteyn, V.S. Study of plasma fluctuations in the Tuman-3m tokamak using microwave reflectometry with an obliquely incident probing beam. *Plasma Phys. Rep.* **2000**, *26*, 813–819. [\[CrossRef\]](#)

10. Conway, G.D.; Schirmer, S.; Klengel, S.; Suttrop, W.; Holzhauer, E.; The ASDEX Upgrade Team. Plasma rotation profile measurements using Doppler reflectometry. *Plasma Phys. Control. Fusion* **2004**, *46*, 951. [\[CrossRef\]](#)
11. Conway, G.D.; Angioni, C.; Dux, R.; Ryter, F.; Peeters, A.G.; Schirmer, J.; Troester, C.; CFN Reflectometry Group; The ASDEX Upgrade team. Observations on core turbulence transitions in ASDEX Upgrade using Doppler reflectometry. *Nucl. Fusion* **2006**, *46*, S799. [\[CrossRef\]](#)
12. Schirmer, J.; Conway, G.D.; Holzhauer, E.; Suttrop, W.; Zohm, H.; The ASDEX Upgrade Team. Radial correlation length measurements on ASDEX Upgrade using correlation Doppler reflectometry. *Plasma Phys. Control. Fusion* **2007**, *49*, 1019. [\[CrossRef\]](#)
13. Happel, T.; Kasperek, W.; Hennequin, P.; Höfler, K.; Honoré, C.; The ASDEX Upgrade Team. Design of a variable frequency comb reflectometer system for the ASDEX Upgrade tokamak. *Plasma Sci. Technol.* **2020**, *22*, 064002. [\[CrossRef\]](#)
14. Hennequin, P.; Honoré, C.; Truc, A.; Quéméneur, A.; Lemoine, N. Doppler backscattering system for measuring fluctuations and their perpendicular velocity on Tore Supra. *Rev. Sci. Instrum.* **2004**, *75*, 3881. [\[CrossRef\]](#)
15. Hennequin, P.; Honoré, C.; Truc, A.; Quéméneur, A.; Fenzi-Bonizet, C.; Bourdelle, C.; Garbet, X.; Hoang, G.T.; The Tore Supra team. Fluctuation spectra and velocity profile from Doppler backscattering on Tore Supra. *Nucl. Fusion* **2006**, *46*, S771. [\[CrossRef\]](#)
16. Hillesheim, J.C.; Peebles, W.A.; Rhodes, T.L.; Schmitz, L.; Carter, T.A.; Gourdain, P.A.; Wang, G. A multichannel, frequency-modulated, tunable Doppler backscattering and reflectometry system. *Rev. Sci. Instrum.* **2009**, *80*, 083507. [\[CrossRef\]](#)
17. Peebles, W.A.; Rhodes, T.L.; Hillesheim, J.C.; Zeng, L.; Wannberg, C. A novel, multichannel, comb-frequency Doppler backscatter system. *Rev. Sci. Instrum.* **2010**, *81*, 10D902. [\[CrossRef\]](#)
18. Oyama, N.; Takenaga, H.; Suzuki, T.; Sakamoto, Y.; Isayama, A.; The JT-60 Team. Density Fluctuation Measurements Using a Frequency Hopping Reflectometer in JT-60U. *Plasma Fusion Res.* **2011**, *6*, 1402014. [\[CrossRef\]](#)
19. Hillesheim, J.C.; Crocker, N.A.; Peebles, W.A.; Meyer, H.; Meakins, A.; Field, A.R.; Dunai, D.; Carr, M.; Hawkes, N.; The MAST Team. Doppler backscattering for spherical tokamaks and measurement of high-k density fluctuation wavenumber spectrum in MAST. *Nucl. Fusion* **2015**, *55*, 073024. [\[CrossRef\]](#)
20. Hillesheim, J.C.; Delabie, E.; Meyer, H.; Maggi, C.F.; Meneses, L.; Poli, E.; JET Contributors. Stationary Zonal Flows during the Formation of the Edge Transport Barrier in the JET Tokamak. *Phys. Rev. Lett.* **2016**, *116*, 065002. [\[CrossRef\]](#)
21. Shi, Z.; Zhong, W.; Yang, Z.; Liang, A.; Wen, J.; Jiang, M.; Shi, P.; Fu, B.; Chen, C.; Liu, Z.; et al. A multiplexer-based multi-channel microwave Doppler backward scattering reflectometer on the HL-2A tokamak. *Rev. Sci. Instrum.* **2018**, *89*, 10H104. [\[CrossRef\]](#) [\[PubMed\]](#)
22. Cabrera, P.M.; Coda, S.; Porte, L.; Offeddu, N.; Lavanchy, P.; Silva, M.; Toussaint, M.; TCV Team. V-band Doppler backscattering diagnostic in the TCV tokamak. *Rev. Sci. Instrum.* **2018**, *89*, 083503. [\[CrossRef\]](#) [\[PubMed\]](#)
23. Hu, J.Q.; Zhou, C.; Liu, A.D.; Wang, M.Y.; Doyle, E.J.; Peebles, W.A.; Wang, G.; Zhang, X.H.; Zhang, J.; Feng, X.; et al. An eight-channel Doppler backscattering system in the experimental advanced superconducting tokamak. *Rev. Sci. Instrum.* **2017**, *88*, 073504. [\[CrossRef\]](#)
24. Wang, M.Y.; Zhou, C.; Liu, A.D.; Zhang, J.; Liu, Z.Y.; Feng, X.; Ji, J.X.; Li, H.; Lan, T.; Xie, J.L.; et al. A novel, tunable, multimodal microwave system for microwave reflectometry system. *Rev. Sci. Instrum.* **2018**, *89*, 093501. [\[CrossRef\]](#) [\[PubMed\]](#)
25. Feng, X.; Liu, A.D.; Zhou, C.; Wang, M.Y.; Zhang, J.; Liu, Z.Y.; Liu, Y.; Zhou, T.F.; Zhang, S.B.; Kong, D.F.; et al. Five-channel tunable W-band Doppler backscattering system in the experimental advanced superconducting tokamak. *Rev. Sci. Instrum.* **2019**, *90*, 024704. [\[CrossRef\]](#) [\[PubMed\]](#)
26. Schmitz, L.; Ruskov, E.; Deng, B.H.; Gota, H.; Gupta, D.; Tuszewski, M.; Douglass, J.; Peebles, W.A.; Binderbauer, M.; Tajima, T. Multi-channel Doppler backscattering measurements in the C-2 field reversed configuration. *Rev. Sci. Instrum.* **2014**, *85*, 11D840. [\[CrossRef\]](#)
27. Kohagura, J.; Tokuzawa, T.; Yoshikawa, M.; Narita, K.; Sakamoto, M.; Nakashima, Y. Doppler Reflectometer System for Measuring Rotation Velocity of Fluctuation in GAMMA 10. *Plasma Fusion Res.* **2016**, *11*, 2402022. [\[CrossRef\]](#)
28. Hacquin, S.; Alper, B.; Sharapov, S.; Borba, D.; Boswell, C.; Fessey, J.; Meneses, L.; Walsh, M.; JET EFDA Contributors. Characterization of Alfvén cascades on the JET tokamak using a multi-channel O-mode reflectometer diagnostic. *Nucl. Fusion* **2006**, *46*, S714. [\[CrossRef\]](#)
29. Lin, Y.; Irby, J.; Stek, P.; Hutchinson, I.; Snipes, J.; Nazikian, R.; McCarthy, M. Upgrade of reflectometry profile and fluctuation measurements in Alcator C-Mod. *Rev. Sci. Instrum.* **1999**, *70*, 1078. [\[CrossRef\]](#)
30. Tokuzawa, T.; Ejiri, A.; Kawahata, K. Multifrequency channel microwave reflectometer with frequency hopping operation for density fluctuation measurements in Large Helical Device. *Rev. Sci. Instrum.* **2010**, *81*, 10D906. [\[CrossRef\]](#)
31. Hornung, G.; Clairet, F.; Falchetto, G.L.; Sabot, R.; Arnichand, H.; Vermare, L. Turbulence correlation properties measured with ultrafast sweeping reflectometry on Tore Supra. *Plasma Phys. Control. Fusion* **2013**, *55*, 125013. [\[CrossRef\]](#)
32. Roh, Y.; Domier, C.W.; Luhmann, N.C., Jr. Ultrashort pulse reflectometry for density profile and fluctuation measurements on SSPX. *Rev. Sci. Instrum.* **2003**, *74*, 1518. [\[CrossRef\]](#)
33. Tokuzawa, T.; Kawahata, K.; Tanaka, K.; LHD Experimental Group. Multichannel ultrashort pulsed radar reflectometer on LHD. *Rev. Sci. Instrum.* **2006**, *77*, 10E903. [\[CrossRef\]](#)

-
34. Domier, C.W.; Zhu, Y.; Dannenberg, J.; Luhmann, N., Jr. C. A next generation ultra short pulse reflectometry (USPR) diagnostic. *Rev. Sci. Instrum.* **2021**, *92*, 034714. [[CrossRef](#)] [[PubMed](#)]
 35. Zhang, B.; Inagaki, S.; Kawachi, Y. Development of a Frequency Comb Sweep Microwave Reflectometer in the Linear Device PANTA. *Plasma Fusion Res.* **2019**, *14*, 1201131. [[CrossRef](#)]